Double transition in a model of oscillating percolation

Sumanta Kundu,[1] Amitava Datta,[2] and S. S. Manna[1]

[1]*Satyendra Nath Bose National Centre for Basic Sciences, Block-JD, Sector-III, Salt Lake, Kolkata-700106, India*

[2]*School of Computer Science and Software Engineering, University of Western Australia, Perth, WA 6009, Australia*

Two distinct transition points have been observed in a problem of lattice percolation studied using a system of pulsating disks. Sites on a regular lattice are occupied by circular disks whose radii vary sinusoidally within $[0, R_0]$ starting from a random distribution of phase angles. A lattice bond is said to be connected when its two end disks overlap with each other. Depending on the difference of the phase angles of these disks, a bond may be termed as dead or live. While a dead bond can never be connected, a live bond is connected at least once in a complete time period. Two different time scales can be associated with such a system, leading to two transition points. Namely, a percolation transition occurs at $R_{0c} = 0.908(5)$ when a spanning cluster of connected bonds emerges in the system. Here, information propagates across the system instantly, i.e., with infinite speed. Secondly, there exists another transition point $R_0^* = 0.5907(3)$ where the giant cluster of live bonds spans the lattice. In this case the information takes finite time to propagate across the system through the dynamical evolution of finite-size clusters. This passage time diverges as $R_0 \to R_0^*$ from above. Both the transitions exhibit the critical behavior of ordinary percolation transition. The entire scenario is robust with respect to the distribution of frequencies of the individual disks. This study may be relevant in the context of wireless sensor networks.

I. INTRODUCTION

The beauty of a percolation model lies in its simplicity as well as nontriviality in studying the order-disorder phase transition [1–3]. A number of variants of the percolation model have been introduced in the last several decades [4–8]. The theory of percolation has been successfully applied to a variety of problems such as metal-insulator transition [9], epidemic spreading in a population [10,11], gelation in polymers [12], wireless communication networks [13–15], etc. The generic feature of all percolation models is the appearance of long-range connectivity from the short-range connectedness when the control variable is tuned to the critical point [16]. The critical points of the percolation models are dependent on the geometry of the system, whereas their critical behavior is characterized by a universal set of critical exponents [1].

Wireless sensor networks (WSNs) [13] are usually composed of sensor nodes which are deployed in a regular topology in the form of a grid for collecting various environmental data, e.g., temperature and humidity. Often a sensor node has a low-powered radio, and limited processing and storage capabilities. Hence it is important that nodes can send collected data to a base station using a multihop radio link through the intermediate nodes in a WSN.

The wireless range of each node is approximately circular and a direct path is established when a node becomes connected to the base station through overlapping wireless ranges of intermediate nodes. This problem is similar to the percolation problem as the base station and a transmitting node become part of a percolating cluster when a radio link is established through overlapping radio transmission ranges of intermediate nodes. It is well known that the wireless ranges of low-power sensor nodes fluctuate temporally due to interference and noise [17–19]. It is important to know when such a percolating path exists as a sensor node can then transmit its packets to the base station without any need for buffering the packets in intermediate nodes, as each sensor node has very little buffer space and packets that cannot be immediately transmitted are usually dropped. Our study of the oscillating percolation problem is an attempt in understanding percolation in the presence of such time-varying transmission ranges. Such temporal variations exist in above-ground [18,19], above-ground to underground [20], and aerial-sensor networks [21]. The speed of variation of these transmission ranges is usually much slower compared to radio transmission speed and hence a percolating cluster persists for a long enough duration for transmitting packets in a WSN.

In this paper, our objective is to model the temporal fluctuations of radio transmission ranges in the WSNs using the framework of percolation theory. Sites of a square lattice are occupied by circular disks of time-varying radii $R(t)$ which pulsate sinusoidally, mimicking the temporal variations of the radio transmission ranges of sensor nodes. Accordingly, a bond between a pair of neighboring sites is considered to be connected if and only if the disks at these sites overlap. Initial assignment of random phase angles of the pulsating disks makes the system heterogeneous. Therefore, the duration of time that a bond remains connected depends on the phases of the two end disks and is different for different bonds. The maximal value of disk radii R_0 is the same for all disks and is the control variable of the problem. In some instants of time the system may be globally connected through the spanning paths of connected bonds between the opposite boundaries of the lattice. In the time-averaged description, the system undergoes a continuous percolation transition for $R_0 > R_{0c}$ for the infinitely large system. Further, for $R_0 < R_{0c}$ when there exists no spanning path, information can still propagate across the system through different finite-size clusters of connected bonds which appear in different instants of time, if longer propagation time is allowed. On average, this transmission time increases as R_0 is decreased and it diverges as $R_0 \to R_0^*$ from above. In the following we present evidence that the system undergoes a second percolation transition at this point. We have studied the critical properties of the system around both the transition points. This study may also be relevant in the context of spreading of epidemic disease in a population,

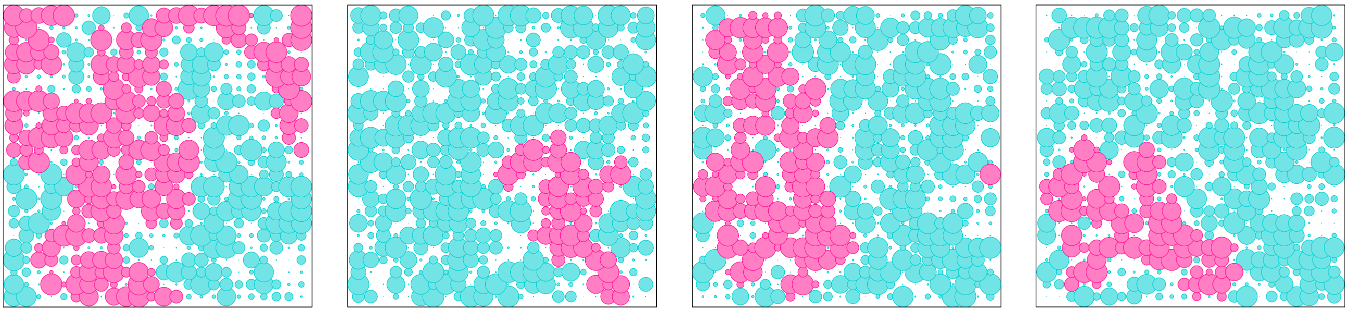

FIG. 1. Snapshots of the time-dependent percolation configuration have been shown on a square lattice of size $L = 24$ with periodic boundary conditions along the horizontal direction. The radii of all the disks having angular frequency $\omega = 1$ pulsate with time as per Eq. (1) and are different at a given time t due to the random initial phases $\{\phi\}$. For $R_0 = 0.85$, the snapshots are taken at $t = 150dt$, $300dt$, $500dt$, and $600dt$ (from left to right), where $dt = \pi/L^2$. The largest cluster painted in magenta (dark grey) sometimes spans the entire lattice and sometimes does not.

spreading of computer viruses through the Internet, and even for rumor spreading in social media, etc.

The paper is organized as follows. We start by describing the model of oscillating percolation in Sec. II. The connectivity properties of lattice bonds are investigated in Sec. III. The calculation of the order parameter and the spanning probability is described in Sec. IV. In Sec. V, we discuss the dependence of the percolation properties on the frequencies of the pulsating disks. In Sec. VI, we have observed the existence of a second percolation transition point defined in terms of two time scales for the speed of information propagation through the connected clusters. In Sec. VII, we generalize the model of oscillating percolation. Finally, we summarize in Sec. VIII.

II. MODEL

A circular disk of radius $R(t)$ that varies with time t has been placed at every site of a square lattice of size $L \times L$ with unit lattice constant. The radii of the disks pulsate periodically following a sinusoidal variation as

$$R(t) = (R_0/2)[\sin(\omega t + \phi) + 1], \tag{1}$$

where R_0 is the control variable that varies in the range [0,1]; the phase ϕ and the angular frequency ω being two parameters. At time $t = 0$, every site is assigned a disk of radius $R(0)$ with a random phase angle drawn from a uniform probability distribution $p(\phi) = 1/2\pi$, $0 \leqslant \phi < 2\pi$. With this only randomness in phase angles, the radii of the disks start pulsating between $[0, R_0]$ following Eq. (1) in a completely deterministic fashion.

A bond between a pair of neighboring disks of radii $R_1(t)$ and $R_2(t)$ is defined to be connected only when

$$R_1(t) + R_2(t) \geqslant 1, \tag{2}$$

which is referred to as the sum rule. The connection status of every bond over a period $T = 2\pi/\omega$ would be repeated *ad infinitum*. A group of sites interlinked through the connected bonds forms a cluster. At a particular time there are several clusters of different shapes and sizes. During the time evolution, sometimes the largest cluster spans the entire lattice and establishes a global connection (Fig. 1). Therefore, within one time period T, the system in general switches between the percolating and nonpercolating states. We define a flag $\eta(t) = 1$ and 0 for the percolating and nonpercolating states, respectively, and its variation is exhibited in Fig. 2. The average residence time in percolating state increases on increasing R_0. To estimate how much the disk configuration becomes different from its initial configuration in time t we define a Hamming distance $\Delta(t) = \max\{|R_i(t) - R_i(0)|\}$ calculated over all sites i which is found to vary as $\Delta(t) = R_0 \sin(\pi t/T)$.

III. CONNECTIVITY OF THE BONDS

The phase difference $\Delta\phi$ between the two pulsating disks at the ends of a bond has a crucial role for the connectivity of the bond. For $R_0 = 1/2$, the bond is connected only at a single instant within the time period T if the disks are in the same phase, whereas, for $R_0 = 1$ the bond remains always connected if the disks are in the opposite phase. This implies that for $1/2 < R_0 < 1$, a bond is connected within a period T only when the phase difference of the two end disks lies within a certain range. The maximum value of the sum $R_1(t) + R_2(t)$ must be $R_0[\cos(\Delta\phi/2) + 1] \geqslant 1$ for the bond to be connected and

$$\Delta\phi = |\phi_2 - \phi_1| \leqslant \Delta\phi_c = 2\cos^{-1}(1/R_0 - 1). \tag{3}$$

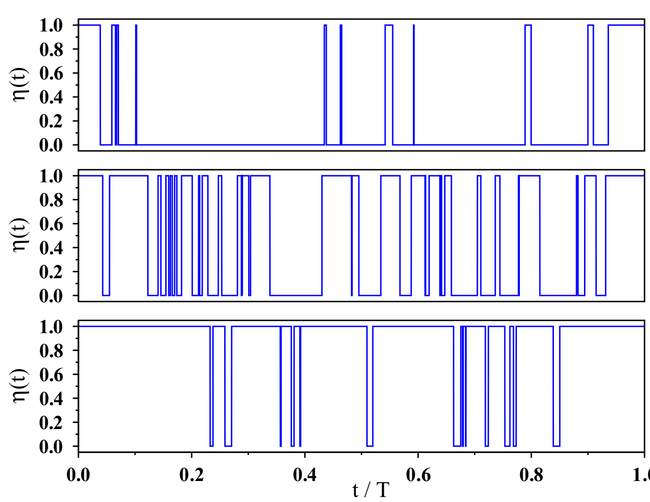

FIG. 2. For $\omega = 1$ and $L = 128$, the phase representing variable $\eta(t)$ has been plotted with t during a period T for $R_0 = 0.88, 0.90$, and 0.92 (from top to bottom). The values of $\eta(t) = 1$ and 0 correspond to the percolating and nonpercolating phases, respectively.

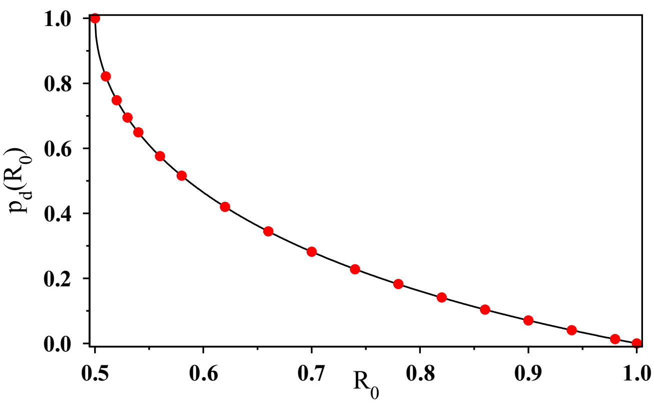

FIG. 3. Plot of the density of dead bonds $p_d(R_0)$ against R_0 which never get connected during the entire time evolution. The numerically obtained data for system size $L = 256$ (filled circles) fit very well with the functional form given in Eq. (5) (solid line).

Evidently, this range increases with increasing the value of R_0. The fraction of time over which a bond remains connected within a period T is given by

$$f_T(R_0,\Delta\phi) = 1/2 - (1/\pi)\sin^{-1}[(1/R_0 - 1)\sec(\Delta\phi/2)]. \tag{4}$$

For a connected bond we must have $f_T(R_0,\Delta\phi) \geqslant 0$ which also gives Eq. (3). For the special case of $R_0 = 1$ and $\Delta\phi = \pi$ we get $f_T = 1$.

This implies that a bond remains unconnected forever if $\Delta\phi > \Delta\phi_c$. We call these bonds the "dead" bonds. In contrast, the remaining set of bonds dynamically changes their connectivity status within a period T and are referred as the "live" bonds. The densities of dead and live bonds are denoted by p_d and p_l, respectively. Expectedly, p_d increases when R_0 is decreased from 1 and it approaches unity as $R_0 \to 1/2$. Since $p(\phi)$ is uniform, the quantity $p_d(R_0)$ is calculated as

$$\begin{aligned} p_d(R_0) &= 1 - 2p(\phi)\Delta\phi_c \\ &= 1 - (2/\pi)\cos^{-1}(1/R_0 - 1). \end{aligned} \tag{5}$$

In Fig. 3, good agreement is observed between the plots of the numerically estimated values of $p_d(R_0)$ against R_0 and the functional form given in Eq. (5).

IV. THE ORDER PARAMETER AND THE SPANNING PROBABILITY

The order parameter $\Omega(R_0,L)$ is defined as the fractional size of the largest cluster, doubly averaged with respect to time between 0 and T and over many initial configurations $\mathcal{C}$ with different sets of random phase angles $\{\phi_i\}$.

$$\Omega(R_0,L) = \langle\langle s_{\max}(R_0,L)\rangle_T\rangle_{\mathcal{C}}/L^2. \tag{6}$$

We also define $\Pi(R_0,L)$ as the spanning probability from the top to the bottom of the lattice.

In numerical simulations time is increased in equal steps of $dt = T/(2L^2)$. A periodic boundary condition has been imposed along the horizontal direction, whereas the global connectivity is checked along the vertical direction as in cylindrical geometry. Both the order parameter $\Omega(R_0,L)$ and the spanning probability $\Pi(R_0,L)$ are estimated for a large number of values of $1/2 < R_0 \leqslant 1$ with a minimum increment of $\Delta R_0 = 0.001$.

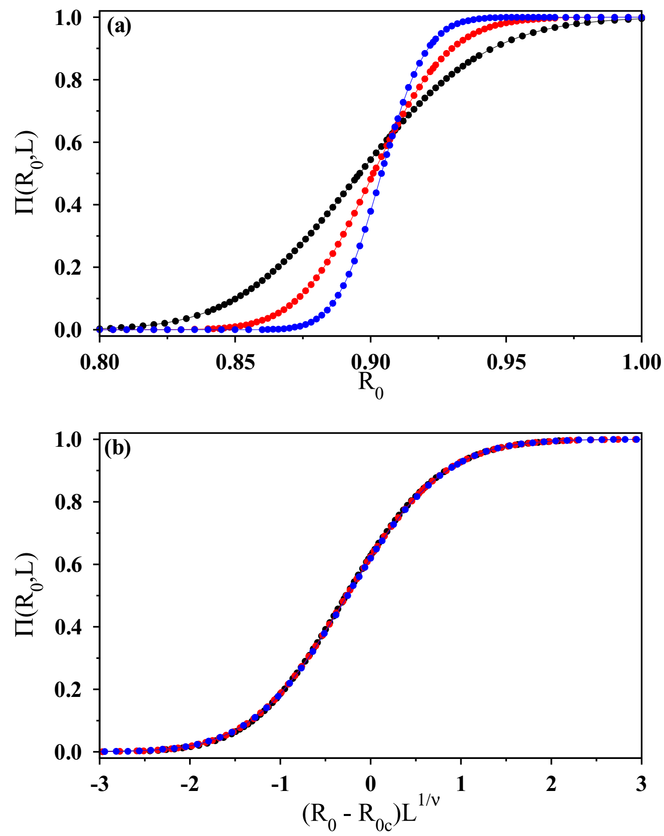

FIG. 4. For $\omega = 1$, and the system sizes $L = 64$ (black), 128 (red), and 256 (blue) (arranged from left to right). (a) The spanning probability $\Pi(R_0,L)$ has been plotted against R_0. (b) Finite-size scaling plot of the same data with $R_{0c} = 0.908(5)$ and $1/\nu = 0.75$ exhibits a very nice data collapse.

In Fig. 4(a), $\Pi(R_0,L)$ has been plotted against R_0 for three different system sizes using $\omega = 1$ for all disks. These curves intersect approximately at the point $[R_{0c},\Pi(R_{0c})]$. We estimate $R_{0c} \approx 0.90$ and the spanning probability $\Pi(R_{0c}) \approx 0.63$, which is quite consistent with the value 0.636 454 001 [22] obtained using Cardy's formula [23]. For a more precise estimation of R_{0c} we define $R_{0c}(L)$ for individual system sizes by $\Pi[R_{0c}(L),L] = 1/2$. The $R_{0c}(L)$ values are estimated by linear interpolation of the data in Fig. 4(a) and then extrapolated to $L \to \infty$ to obtain R_{0c}. Tuning the value of R_{0c} the difference $R_{0c} - R_{0c}(L)$ has been plotted against $L^{-1/\nu}$ to obtain the best value of $R_{0c} = 0.908(5)$. Here $\nu = 4/3$, the correlation length exponent of ordinary percolation. Further, for a finite-size scaling plot $\Pi(R_0,L)$ has been plotted against $(R_0 - R_{0c})L^{1/\nu}$. An excellent data collapse for all three system sizes in Fig. 4(b) indicates the finite-size scaling form

$$\Pi(R_0,L) \sim \mathcal{G}[(R_0 - R_{0c})L^{1/\nu}]. \tag{7}$$

A similar analysis has been performed for the order parameter $\Omega(R_0,L)$. Figure 5(a) shows $\Omega(R_0,L)$ against the R_0 plot for the same three system sizes and their finite-size scaling analyses have been done in Fig. 5(b), indicating the scaling

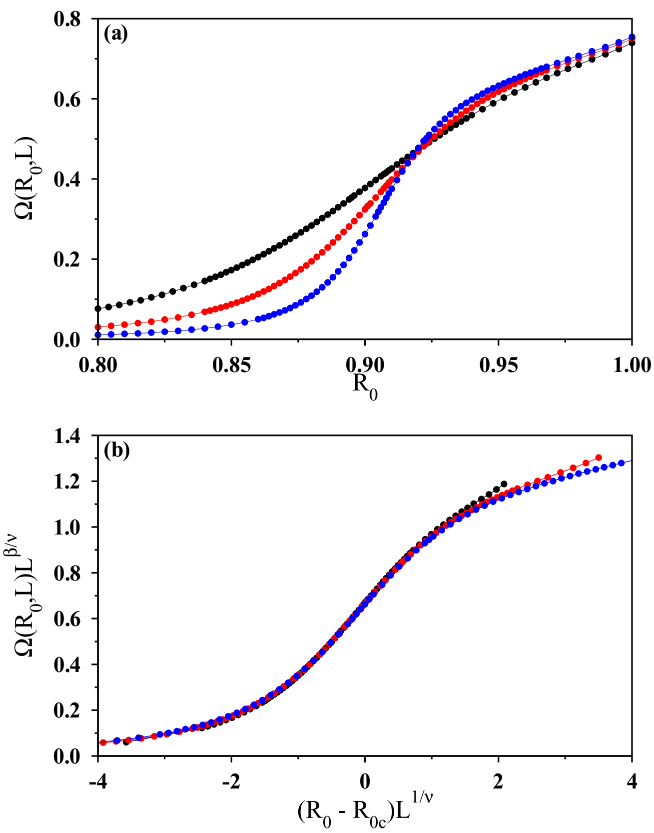

FIG. 5. For $\omega = 1$, (a) variation of the order parameter $\Omega(R_0, L)$ as defined in Eq. (6) with R_0 has been shown for the system sizes $L = 64$ (black), 128 (red), and 256 (blue) (arranged from left to right); (b) finite-size scaling of the same data using $R_{0c} = 0.908(5)$, $1/\nu = 0.75$, and $\beta/\nu = 0.114(5)$ exhibits an excellent data collapse.

form

$$\Omega(R_0, L)L^{\beta/\nu} \sim \mathcal{F}[(R_0 - R_{0c})L^{1/\nu}]. \quad (8)$$

From this scaling we get $\beta/\nu = 0.114(5)$ compared to the exact value of $\beta/\nu = 5/48 \approx 0.1042$ with $\beta = 5/36$ [1] for ordinary percolation.

V. PERCOLATION WITH DISTRIBUTED FREQUENCIES

Now we consider the situation where each disk is randomly assigned a frequency ω_1 with probability f and frequency ω_2 with probability $1 - f$ with previously prescribed random phase angles. The time period $T_{(\omega_1,\omega_2)}$ has been calculated numerically for a large number of pairs of angular frequencies, where the frequencies are the rational numbers. Since for two rational numbers a/b and c/d, $\mathrm{HCF}(a/b, c/d) = \mathrm{HCF}(a,c)/\mathrm{LCM}(b,d)$, HCF and LCM being the highest common factor and lowest common multiplier, respectively, we find the following functional form

$$T_{(\omega_1,\omega_2)} = 2\pi/\mathrm{HCF}(\omega_1, \omega_2) \quad (9)$$

which is independent of $0 < f < 1$. A generalized form of the above expression for T can further be given for the mixture of N distinct frequencies $\omega_1, \omega_2, \ldots, \omega_N$ as

$$T_{(\omega_1,\omega_2,\ldots,\omega_N)} = 2\pi/\mathrm{HCF}(\omega_1, \omega_2, \ldots, \omega_N). \quad (10)$$

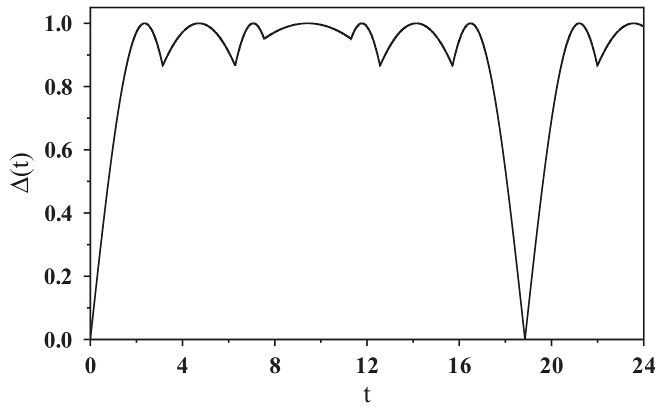

FIG. 6. Plot of $\Delta(t)$ against t for $L = 64$, $R_0 = 1$, and only for one initial configuration. The system is composed of three different types of disks characterized by their own frequencies: $\omega_1 = 1/3$, $\omega_2 = 2/3$, and $\omega_3 = 4/3$. Here, we find that the minimum value of $\Delta(t) = 2.96 \times 10^{-4}$ is at $t = 18.85$. The numerical estimate of $T = 18.85$ matches considerably well with the value of $T = 6\pi$ calculated using Eq. (10).

This formula has been numerically verified using the mixtures up to five distinct frequencies. For example, the time period is estimated using the plot of $\Delta(t)$ against t in Fig. 6 for three distinct frequencies.

This model is further extended by assigning a distinct frequency to each disk drawing them from a uniform distribution $p(\omega)$ between [0,1]. In this case, T is very large and therefore we run the simulations up to $t = 10\pi$, in steps of $dt = 2\pi/(2L^2)$. Surprisingly, the critical point $R_{0c} = 0.908(5)$, the crossing probability ≈ 0.63, and the set of critical exponents remain unaltered within our numerical accuracy, i.e., they do not depend on the actual number of distinct frequencies.

Here, we put forward an explanation for this frequency independence. Let $p(R)$ be the probability distribution of the radii of the disks which we argue to be independent of time using Eq. (1). Introducing a variable $Q = \omega t$, the joint distribution function $p(Q,R)$ can be expressed in terms of the distribution functions of the two mutually independent variables Q and ϕ as, $p(Q,R) = p(\omega t)p(\phi)|J(Q,R)|$, where $J(Q,R)$ is the Jacobian of the transformation. Finally, the marginal distribution of R is calculated from $p(Q,R)$ and has the form

$$p(R) = 1/(\pi\sqrt{RR_0 - R^2}), \quad (11)$$

independent of the distribution of $p(\omega)$. This result can be compared for a system having a uniform distribution of disk radii between $[0, R_0]$, where the transition occurs at $R_{0c} = 0.925(5)$ [24]. Equation (11) has been verified numerically and the matching is very good (not shown here). Using this equation one can calculate the probability that a bond is connected by the sum rule. Equating this probability to 1/2, the random bond percolation threshold, and neglecting local correlations one obtains an approximate estimate of $R_{0c} = 1$.

VI. THE SECOND PERCOLATION TRANSITION

In this section we exhibit that a second percolation transition exists in terms of the passage time for information propagation.

For this description we consider that information propagates with infinite speed within a cluster of connected bonds, i.e., spreads instantly to all sites of the cluster irrespective of the site of its introduction. This implies that for $R_0 > R_{0c}$ there exists a spanning cluster across the system through which information can be transmitted at the same time instant from one side of the system to its opposite side. On the other hand, for $R_0 < R_{0c}$ there are finite isolated clusters of connected bonds which dynamically change their shapes and sizes.

Now we introduce the second mechanism for information propagation. We assume that the sites of an isolated informed cluster of connected bonds retain the information with themselves forever. In a later time during the time evolution, this informed cluster may merge with another uninformed cluster and information would then propagate instantly to the sites of the new cluster. It is therefore apparent that if one waits long enough, maybe several multiples of the time period T, it is likely that information would propagate through the system even when $R_0 < R_{0c}$. More elaborately, all sites at the top row of the square lattice are given some information at time $t = 0$. This information is instantly transmitted to all sites of all clusters that have at least one site on the top row. All these sites are now informed sites and they keep the information with them. Since time is increased in steps of dt, at the next time step the status of every bond is freshly determined and some new sites (clusters) may get linked to these informed sites through a fresh set of connected bonds. Immediately, the information is transmitted again to all sites of all these clusters. In this way the information spreads to more and more sites of the entire lattice. Sometimes it may happen that the spreading process pauses for a few time steps, although the statuses of different bonds are still changing. We assume that the spreading process terminates permanently when the information reaches the bottom of the lattice. The time required on average for this passage is denoted by $T_I(R_0,L)$. Since the average number of connected bonds in the system decreases when the value of R_0 is decreased, this average information passage time increases. Finally, $T_I(R_0,L)$ diverges when R_0 approaches R_0^* from above. Therefore, we recognize R_0^* as the second critical point of percolation transition.

In general for $R_0 > 1/2$, the live and dead status of all bonds of the lattice are determined. This gives a frozen configuration of live and dead bonds for every initial configuration of random phase angles. Only the live bonds can take part in the information propagation, and therefore, for a global passage of information across the system, it is necessary that the system must have a spanning cluster of live bonds. This leads us to identify the critical point R_0^* as the configuration averaged minimum value of R_0 when a spanning cluster of live bonds appears in the system. Numerically, the precise value of R_0^* has been estimated using the bisection method. We started with a pair of values of R_0, namely, $R_0^{\rm hi}$ and $R_0^{\rm low}$, corresponding to the globally connected and disconnected system, respectively, through the live bonds. This interval is iteratively bisected until it becomes smaller than a preassigned tolerance value of 10^{-7}. Averaging over a large number of independent configurations $R_0^*(L)$ for the system size L is estimated. The entire procedure

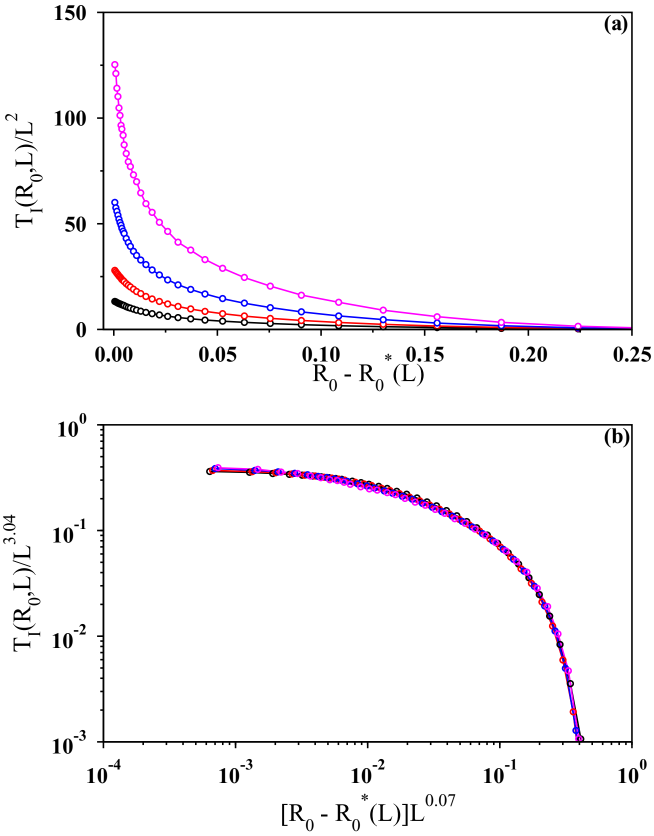

FIG. 7. (a) Average passage time for information propagation $T_I(R_0,L)/L^2$ has been plotted against the deviation from the critical point $R_0 - R_0^*(L)$ for $L = 32$ (black), 64 (red), 128 (blue), and 256 (magenta) (arranged from bottom to top) using $\omega = 1$ for all the disks. As $R_0 \to R_0^*(L)$, the time $T_I(R_0,L)$ diverges. (b) A scaling by $T_I(R_0,L)/L^{3.04}$ against $[R_0 - R_0^*(L)]L^{0.07}$ exhibits a good data collapse.

is then repeated for several values of L and extrapolated to $L \to \infty$ to obtain $R_0^* = R_0^*(\infty)$. We find that the usual extrapolation method using $L^{-1/\nu}$ works very well here as well with $\nu = 4/3$. Our best estimate for the critical point is $R_0^* = 0.5907(3)$.

The average information propagation time $T_I(R_0,L)/L^2$ has been plotted against $R_0 - R_0^*(L)$ in Fig. 7(a) for four different system sizes using $\omega = 1$ for all the disks. It is observed that as R_0 approaches R_0^*, the propagation time becomes increasingly larger. Further, for a specific value of R_0, the propagation time increases with the system size. In Fig. 7(b) the scaled plot of the same data has been exhibited. A data collapse is obtained when $T_I(R_0,L)/L^{3.04}$ has been plotted against $[R_0 - R_0^*(L)]L^{0.07}$. This is consistent with the variation of the largest passage time which grows as $T_I(R_0^*,L) \sim L^{3.08}$.

To characterize precisely the second transition point in terms of the live bonds, we have also estimated the fractal dimension d_f of the largest cluster of live bonds, the exponent γ for the second moment of the cluster size distribution at R_0^*, and the order parameter exponent β around R_0^*. These exponents are very much consistent with the ordinary percolation exponents in two dimensions.

An approximate estimate of the critical point R_0^* can also be made neglecting the local correlations. At the transition point, the density of live bonds $p_l(R_0^*)$ is equated to $1/2$, the random bond percolation threshold on the square lattice. Using Eq. (5) we obtain $R_0^* = 2/(2+\sqrt{2}) \approx 0.5858$, which is very close to our numerically obtained value of $R_0^* = 0.5907(3)$.

VII. GENERALIZED OSCILLATING PERCOLATION

In this section we have generalized our model by introducing a shift parameter that enhances the disk radii by an amount R_s. Therefore, the radius of a disk sinusoidally varies between R_s and $R_0 + R_s$ as

$$R(t) = R_s + (R_0/2)[\sin(\omega t + \phi) + 1]. \tag{12}$$

For a specific value of R_s, it is now more likely that the radii of the end disks of a bond would satisfy the sum rule. Therefore the density of connected bonds at any given instant of time t gets enhanced. As a consequence, the value of the critical amplitude $R_{0c}(R_s)$ decreases from its value R_{0c} for $R_s = 0$.

Variation of the order parameter $\Omega(R_0, R_s, L)$ has been studied against R_0 for three different shifts R_s. For each R_s three different system sizes L have been exhibited in Fig. 8(a).

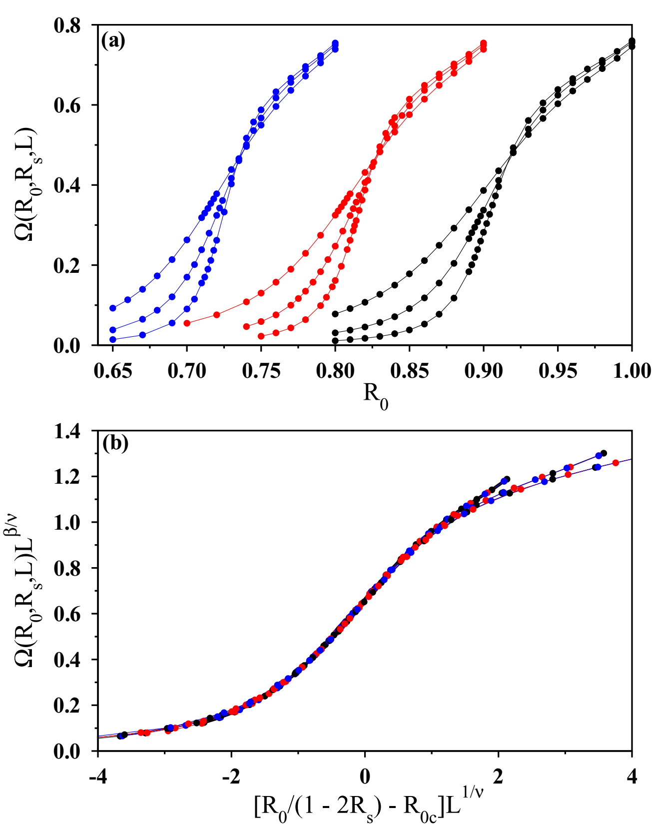

FIG. 8. For $R_s = 0.001$ (black), 0.05 (red) and 0.1 (blue) (arranged from right to left), and for $L = 64$, 128 and 256 for each R_s. (a) The variation of the order parameter $\Omega(R_0, R_s, L)$ with R_0 has been shown using $\omega = 1$ for all the disks. (b) The same data as in (a) has been scaled suitably. A scaling by $\Omega(R_0, R_s, L)L^{\beta/\nu}$ against $[R_0/(1-2R_s) - R_{0c}]L^{1/\nu}$ with $R_{0c} = 0.908(5)$, $1/\nu = 0.75$ and $\beta/\nu = 0.112(5)$, exhibiting a nice data collapse.

Using the same data, in Fig. 8(b) we show the scaling form

$$\Omega(R_0, R_s, L)L^{\beta/\nu} \sim \mathcal{F}[(R_0/(1-2R_s) - R_{0c})L^{1/\nu}] \tag{13}$$

for the order parameter works very well with $R_{0c} = 0.908(5)$. The best data collapse is obtained using $1/\nu = 0.75$ and $\beta/\nu = 0.112(5)$. Again, the finite-size scaling exponents closely match with the exponents of the ordinary percolation in two dimensions.

From Fig. 8(b) equating $[R_0/(1-2R_s) - R_{0c}]L^{1/\nu} = 0$ one gets

$$R_{0c}(R_s) = (1 - 2R_s)R_{0c}. \tag{14}$$

Numerical values of $R_{0c}(R_s)$ are in very good agreement with those obtained from Eq. (14). The shift R_s effectively reduces the lattice constant by an amount $2R_s$. This explains the origin of the factor $(1 - 2R_s)$ in Eq. (14).

VIII. SUMMARY

We have formulated a percolation model using a collection of pulsating disks keeping in mind the global connectivity properties of the wireless sensor networks in the presence of temporal fluctuations of radio transmission ranges. Every site of a regular lattice is occupied by a circular disk which pulsates sinusoidally within $[0, R_0]$. The initial state is characterized by the random phase angles of the pulsating disks. Further, a lattice bond is said to be connected as long as the pair of end disks overlap. The maximal radius R_0 acts as the control variable whose value is tuned continuously to change the fraction of the connected bonds in the system. The first transition takes place at $R_{0c} = 0.908(5)$ when the giant cluster of connected bonds spans the entire system. It is imagined that the information passes through the spanning cluster instantly, i.e., with infinite speed for all $R_0 > R_{0c}$. Moreover, the information can even transmit through the system when there are only isolated finite-size clusters of connected bonds for $R_0 < R_{0c}$. This happens when informed clusters come in contact with the uninformed clusters and pass the information. Such transmission takes a finite time to cover the system and it diverges when R_0 approaches R_0^* from above; $R_0^* = 0.5907(3)$ marks the second transition point. A consideration of the phase differences between the end disks of bonds allows one to classify all bonds in terms of dead and live. Dead bonds can never be connected, whereas the live bonds are connected at least once within one period. Interestingly, we could recognize R_0^* to be the transition point when the global connectivity through the spanning cluster of live bonds first appears in the system. Expectedly, both the transitions exhibit the critical behavior of ordinary percolation transition since the interaction is short ranged.

For future investigations, one can generalize this model by placing the centers of the pulsating disks at random positions on a continuous plane by a Poisson process, like in continuum percolation [3,25,26].

ACKNOWLEDGMENT

We thankfully acknowledge R. M. Ziff for his valuable comments and critical review of the manuscript.

[1] D. Stauffer and A. Aharony, *Introduction to Percolation Theory* (Taylor & Francis, London, 2003).

[2] G. Grimmett, *Percolation* (Springer, New York, 1999).

[3] R. Meester and R. Roy, *Continuum Percolation* (Cambridge University Press, Cambridge, UK, 1996).

[4] N. Araùjo, P. Grassberger, B. Kahng, K. J. Schrenk, and R. M. Ziff, Eur. Phys. J.: Spec. Top. **223**, 2307 (2014).

[5] A. A. Saberi, Phys. Rep. **578**, 1 (2015).

[6] D. Lee, Y. S. Cho, and B. Kahng, J. Stat. Mech. (2016) 124002.

[7] D. Achlioptas, R. M. D'Souza, and J. Spencer, Science **323**, 1453 (2009).

[8] A. Coniglio, H. E. Stanley, and W. Klein, Phys. Rev. Lett. **42**, 518 (1979).

[9] L. de Arcangelis, S. Redner, and H. J. Herrmann, J. Phys. Lett. **46**, 585 (1985).

[10] P. Grassberger, Math. Biosci. **63**, 157 (1983).

[11] M. E. J. Newman, Phys. Rev. E **66**, 016128 (2002).

[12] P. J. Flory, J. Am. Chem. Soc **63**, 3096 (1941).

[13] W. Dargie and C. Poellabauer, *Fundamentals of Wireless Sensor Networks: Theory and Practice* (Wiley, New York, 2010).

[14] I. Glauche, W. Krause, R. Sollacher, and M. Greiner, Physica A **325**, 577 (2003).

[15] W. Krause, I. Glauche, R. Sollacher, and M. Greiner, Physica A **338**, 633 (2004).

[16] M. Sahimi, *Applications of Percolation Theory* (Taylor & Francis, London, 1994).

[17] R. Sollacher, M. Greiner, and I. Glauche, Wirel. Netw. **12**, 53 (2006).

[18] N. Baccour, A. Kouba, L. Mottola, M. Ziga, H. Youssef, C. Boano, and M. Alves, ACM Trans. Sens. Netw. **8**, 34 (2012).

[19] N. Baccour, A. Kouba, H. Youssef, and M. Alves, Ad Hoc Netw. **27**, 1 (2015).

[20] B. Silva, R. Fisher, A. Kumar, and G. Hancke, IEEE Trans. Ind. Inf. **11**, 1099 (2015).

[21] N. Ahmed, S. Kanhere, and S. Jha, IEEE Commun. Mag. **54**, 52 (2016).

[22] R. M. Ziff, Phys. Rev. E **83**, 020107(R) (2011).

[23] J. Cardy, J. Stat. Phys. **125**, 1 (2006).

[24] S. Kundu and S. S. Manna, Phys. Rev. E **93**, 062133 (2016).

[25] E. T. Gawlinski and H. E. Stanley, J. Phys. A **14**, L291 (1981).

[26] J. Quintanilla, Phys. Rev. E **63**, 061108 (2001).